Study on Multipath Effect of GEO Satellite in BeiDou Navigation Satellite System

Peng Wu, Baowang Lian, Yulong Song and Zhe Yue

Abstract For BeiDou navigation satellite system, multipath fading from geostationary Earth orbit (GEO) satellites constraints BeiDou receiver to provide a high-precision positioning service, which is not negligible. By designing multipath fading mathematical model, the mechanism of multipath fading is analyzed. This paper proposes a method, by analyzing the fading trend of the first nulling point and second nulling point of Kepler multipath fading (KMPF) factor, which can reflect variation trend of the multipath error of GEO. Finally, the simulation results verify that the KMPF factor provides an important method to analyze the GEO multipath errors.

Keywords BeiDou GEO satellites · Multipath effect · Kepler multipath fading factor

1 Introduction

The satellite navigation receiver provides PNT information to the user by measuring the pseudorange of the navigation signal. The pseudorange measurement is vulnerable to various errors, which decrease the positioning accuracy of the receiver. The impact of the atmosphere on the navigation signal is characterized by an atmospheric delay, which includes ionospheric delay and tropospheric delay, when the navigation signals transit atmosphere. Besides, the satellite navigation receiver may also suffer from the multipath signal generated by the surrounding environment, which arises loop tracking errors, and ultimately affects the positioning accuracy. In addition, for navigation system, there also exist other unignored errors, such as satellite clock error, ephemeris errors, receiver clock, and so on. Due to each error, source performs the different characteristics in time domain or frequency domain, the corresponding methods can be used to reduce or even eliminate the errors. The common errors

P. Wu (✉) · B. Lian · Y. Song · Z. Yue
School of Electronics and Information, Northwestern Polytechnical University, 710072 Xi'an, China
e-mail: wupengrock@163.com

J. Sun et al. (eds.), *China Satellite Navigation Conference (CSNC) 2016 Proceedings: Volume III*, Lecture Notes in Electrical Engineering 390,
DOI 10.1007/978-981-10-0940-2_31

resulting from atmospheric delay, satellite ephemeris error, and satellite clock error can be greatly eliminated by differential approach or be remarkably improved by building the corresponding mathematical model. However, the multipath errors cannot be removed by differential technique since multipath is closely related to the environment around the antenna and it is hard to achieve correlation for receivers at different locations. So, the investigation for the mechanism of multipath signal and the mitigation methods has vital significance to reduce the observation errors and to improve the positioning accuracy. For instance, code measurements are used for estimation of atmospheric delay and calculation of satellite orbit parameters in GNSS control segment. If multipath signal infects the code measurements, then the positioning accuracy and timing performance are both directly decreased. Therefore, the influence of multipath error on the navigation system must be paid high attention.

To study the GEO satellites' contribution for improving the system positioning accuracy in Wide Area Augmentation System (WAAS), [1] proposes that "standing multipath" is a main constraint to make WAAS get better performance. Reference [2] shows that even though GEO satellites are not only used for data link to sent correction and integrity messages, but also to be used as additional ranging sources in WAAS, they have a lower ranging accuracy compared with GPS satellites, and multipath is a crucial interference factor for ranging errors. In Refs. [3] and [4], authors research that the multipath fading characteristics of MEO satellites in GPS are much different from multipath fading characteristics of GEO satellites, which indicates that the multipath fading characteristics are closely related with the satellite orbit.

At present, the research on the mechanism of GEO satellite multipath effect is still not sufficient, nevertheless the elimination algorithms for GPS satellites have been studied very deeply. These algorithms provide an effective way to study the multipath effect of GEO satellite in the BeiDou navigation system. Duo to the GEO satellite, location is almost stationary relative to the Earth, the multipath interference varies very slowly with time. Recently, Ref. [5] presents that the GEO multipath interference has more destructive ability than IGSO satellites and MEO satellites.

To solve this problem, this paper acquires the analytic formula of the multipath frequency fading by establishing the ground multipath reflection model. Subsequently, according to the geometric relations between the satellite and the receiver, as well as the theory of coordinate transformation, the Kepler multipath fading (KMPF) factor has been derived, which can reflect the multipath error caused by the satellite orbit parameters. Finally, simulation results verify the analysis on the mechanism of GEO satellite multipath effects.

2 Multipath Fading Mathematical Model

To characterize the influence of multipath signal, it is assumed that the antenna receives a direct signal and a reflected signal simultaneously, then the compound signal $s(t)$ can be expressed as

$$s(t) = \mathrm{Ap}(t)\sin(\omega_0 t) + \alpha \mathrm{Ap}(t - \tau_\mathrm{m})\sin(\omega_0 t + \Delta\Phi_\mathrm{m}(t)) \quad (1)$$

where A denotes the signal amplitude, ranging and data codes are denoted by $p(t) = \pm 1$, ω_0 is the angular frequency including the Doppler shift $\Delta\omega_0 = 2\pi\Delta f_0$, α is the attenuation coefficient of reflected signal, τ_m is the multipath delay, $\Delta\Phi_\mathrm{m}(t) = \Delta\varphi_\mathrm{m} + (\Delta\omega_\mathrm{m} - \Delta\omega_0)t$ denotes the multipath relative phase, where $\Delta\varphi_\mathrm{m}$ is multipath initial phase, and $(\Delta\omega_\mathrm{m} - \Delta\omega_0)$ is the Doppler difference between the direct and the multipath signal. Duo to the satellites, movement is relative to the antenna phase center, the multipath delay τ_m and carrier phase $\Delta\Phi_\mathrm{m}(t)$ vary with time, and the multipath carrier frequency generates an increment that is multipath fading frequency and can be expressed as follows:

$$\Delta f_\mathrm{m} = \frac{1}{2\pi}\frac{\mathrm{d}\Delta\Phi_\mathrm{m}(t)}{\mathrm{d}t} = \frac{1}{2\pi}\frac{\mathrm{d}[\Delta\varphi_\mathrm{m} + (\Delta\omega_\mathrm{m} - \Delta\omega_0)t]}{\mathrm{d}t} \quad (2)$$

According to Eq. (2), the rate of Doppler difference $(\Delta\omega_\mathrm{m} - \Delta\omega_0)$ determines the frequency of the occurring multipath variations. Ideally, since the GEO satellites is stationary to the Earth, the multipath relative phase turns into a constant and the term $(\Delta\omega_\mathrm{m} - \Delta\omega_0)$ becomes zero. Meanwhile, because of the static behavior of the multipath relative phase, the multipath observation will show a fixed bias [6].

As mentioned above, the multipath fading characteristics are determined by the Doppler difference between direct and reflected signals. In other words, the geometry between satellite orbit and reflection point influences multipath effects. Then, we will analyze the GEO satellites multipath fading characteristics by using ground multipath reflection model.

Figure 1 shows the ground multipath reflection model in which the multipath extra-traveled distance $L_\mathrm{m}(t)$ can be expressed as a function of the satellite elevation

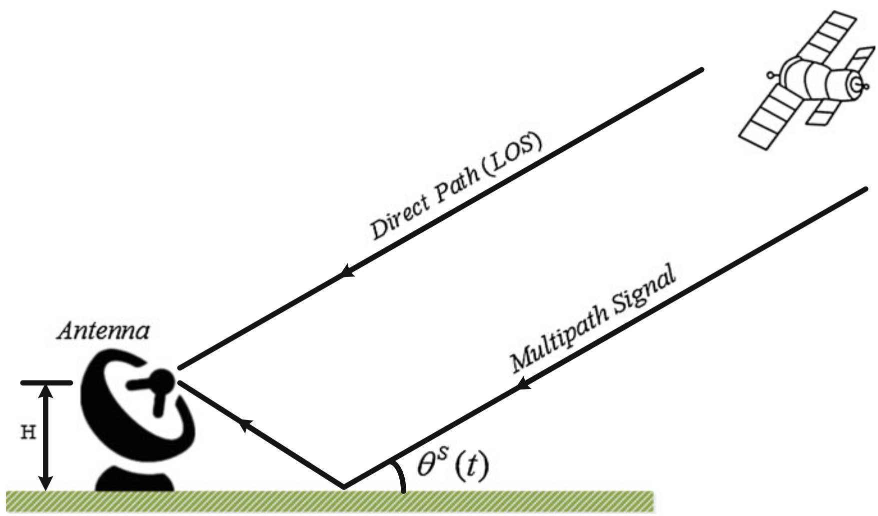

Fig. 1 Model of ground multipath

$\theta^s(t)$, and the height H of the receiver antenna phase center above the reflecting surface at time t. So, we have

$$L_{\mathrm{m}}(t) = 2H \cdot \sin\theta^s(t) \tag{3}$$

According to Eq. (3), the multipath delay of static receiver is closely related to the satellite elevation. In satellite navigation system, the satellite elevation is time-varying relative to the receiving antenna, even for the BeiDou GEO satellites, the elevation could not keep constant over the time. In term of the electromagnetic wave propagation theory, the carrier multipath relative phase can be expressed as

$$\Delta\Phi_{\mathrm{m}}(t) = 2\pi\frac{L_{\mathrm{m}}(t)}{\lambda} = \frac{4\pi H \cdot \sin\,\theta^s(t)}{\lambda} \tag{4}$$

where the λ is wavelength of the signal.

Substituting Eq. (4) into Eq. (2), and assuming that the receiving antenna and surroundings around the antenna are keeping relatively static, then the multipath fading frequency of the ground multipath reflection model can be expressed as

$$\Delta f_{\mathrm{m}}(t) = \frac{1}{2\pi}\frac{\mathrm{d}\Delta\Phi_{\mathrm{m}}(t)}{\mathrm{d}t} = \frac{2H}{\lambda}\frac{\mathrm{d}[\sin\theta^s(t)]}{\mathrm{d}t}. \tag{5}$$

3 Analysis of the Multipath Parameters

Figure 2 illustrates the geometry between Earth and satellite orbit in the Earth-centered, Earth-fixed (ECEF) system, in which o, R_e, S, $r(t)$, R^s, and A stand for Earth's center, Earth's radius, satellite position, the distance between the satellite and receiver $\|AS\|$, geocentric distance of satellite orbit $\|OS\|$, and location of receiving antenna (A is not the North Pole, but it represents the position of any position on the Earth surface. In order to comply with the visual habits, it points to the zenith direction) at time t, respectively. Besides, plane P is a tangential plane of the Earth surface at point A, as Fig. 2 shows, point D is the projection of satellite S on plane P, and the elevation $\theta^s(t)$ is an included angle between the vector AS and the vector AD. In order to facilitate the geometric relationships among these vectors in Fig. 1, these vectors are presented on a two-dimensional plane as shown in Fig. 1, and according to the law of cosines, we have

$$\sin\theta^s(t) = \frac{R^{s2} - R_e^2 - r^2(t)}{2R_e r(t)} \tag{6}$$

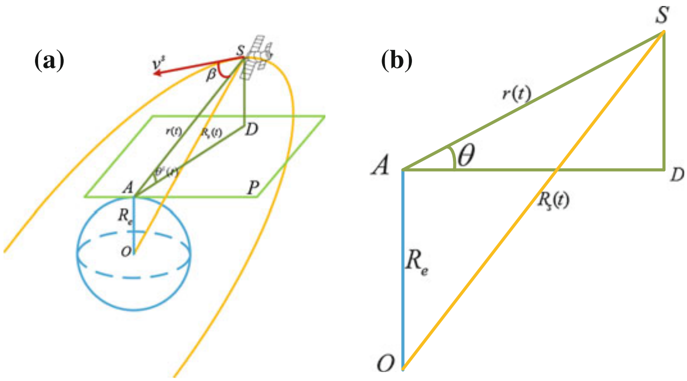

Fig. 2 Geometry between Earth and the satellite orbit. **a** 3D geometry between Earth and satellite orbit, **b** section plan for (**a**)

and substituting Eq. (6) into Eq. (5), the multipath fading frequency is given by

$$\Delta f_{\mathrm{m}}(t) = -\frac{2H}{\lambda}\left(\frac{1}{R_e} + \frac{\sin\theta^s(t)}{r(t)}\right)r'(t) \tag{7}$$

In this equation, the elevation and the distance between satellite and receiver can be extracted from the observables, therefore the characteristic of the multipath fading is mainly restricted by r' at time t. Actually, $r'(t)$ reflects the rate of distance change between satellite and receiver and it is proportional to relative speed along the signal propagation direction. In the ECEF frame, v^s, v, and $\boldsymbol{1}^s$ are the speed of satellite, the speed of receiver, and satellite unit observation vector at the receiver, respectively, thus $r'(t)$ is the dot product of v^s and v, namely

$$\mathbf{r}' = (\mathbf{v^s} - \mathbf{v}) \cdot \boldsymbol{1}^s = (\upsilon^s - \upsilon)\cos\beta \tag{8}$$

where β is the included angle between $(v^s - v)$ and $\boldsymbol{1}^s$, which is given by

$$\left[\cos\beta = \frac{e\sin f^s}{\sqrt{1+e^2+2e\cos f^s}}\cos\alpha\right] \tag{9}$$

In this equation, $\alpha = \langle SA, SO\rangle$, f^s is the true anomaly. For static scenario, the receiver's speed is zero, then A is the angle between v^s and $\boldsymbol{1}^s$, as shown in Fig. 2b. Based on the analysis of Eqs. (7)–(9), the multipath fading characteristic of static receiver is closely related with the speed of satellite v^s and β.

4 Kepler Multipath Fading Factor

4.1 Derivation of KMPF

As mentioned above, the multipath fading characteristic $\Delta f_{\mathrm{m}}(t)$ is closely associated with the satellite's speed v^s and β. Therefore, the satellite's speed will be as a entry point to further analyze the relationship between the satellite orbit parameters and multipath fading frequency.

Figure 3 depicts the Kepler parameters of satellite orbit, where i is the inclination angle, Ω_0 is the longitude of ascending node, ω is the argument of perigee, $f^s = \omega^s t$ is the true anomaly at time t, and ω^s is the angular rate of the satellite in the Earth-centered, inertial (ECI) coordinate system, which can be achieved from ephemeris. Then, based on the scheme to transform the coordinate systems, the speed of satellite in ECEF system can be calculated as follows:

$$v^s = \frac{R^s}{\sqrt{2}} V \tag{10}$$

where

$$V = \sqrt{(\omega_e^2 + \omega^{s2})(1 + \cos^2 i) - 4\omega_e \omega^s \cos^2 i + [\omega_e^2 \cos(2\omega^s t + 2\omega) + \omega^{s2}]\sin^2 i} \tag{11}$$

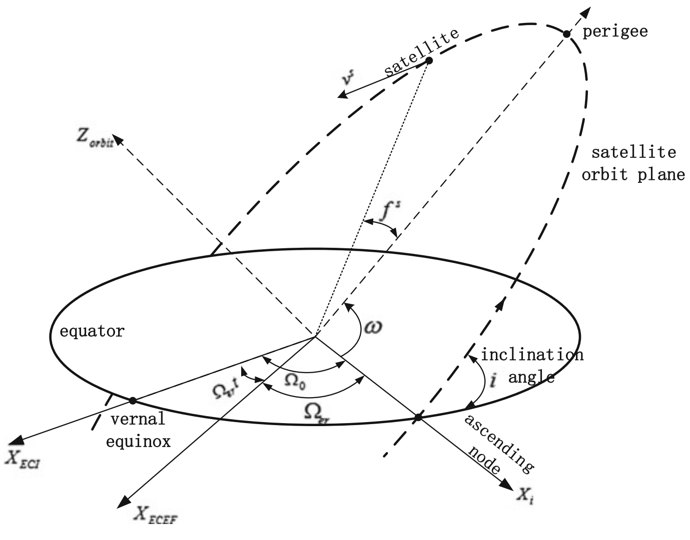

Fig. 3 Kepler parameters of satellite orbit

Meanwhile, according to Eqs. (8) and (9), the Kepler multipath fading factor can be defined as follows:

$$\left[\kappa(t) \triangleq \frac{e\sin f^s}{\sqrt{1+e^2+2e\cos f^s}} V\cos\alpha\right] \tag{12}$$

This equation includes some orbit parameters such as the eccentricity of the satellite orbit e, the inclination angle i, and so on. Subsequently, a deep analysis of these orbit parameters will be discussed in the next section.

4.2 Analysis of KMPF Simulation Curve

4.2.1 Influence of the Orbit Inclination *i* and Eccentricity *e* on KMPF

The inclination of GEO satellites in BeiDou system is roughly in the range of 0.03 to 0.09°, and the GEO satellites inclination in WAAS system has a better performance whose range is from 0.01° to 0.02°. In addition, in order to understand deeply the impact of inclination on KMPF, the simulation still takes the situation into consideration when the inclinations are 0.001° and 0.0001°, respectively, as shown in Fig. 4. Meanwhile, some features can be concluded from the curves in Fig. 4.

(i) All the curves show the first nulling at around 11 h.
(ii) When $i = 0.001°$, the amplitude of KMPF factor is greater than others at the first nulling.

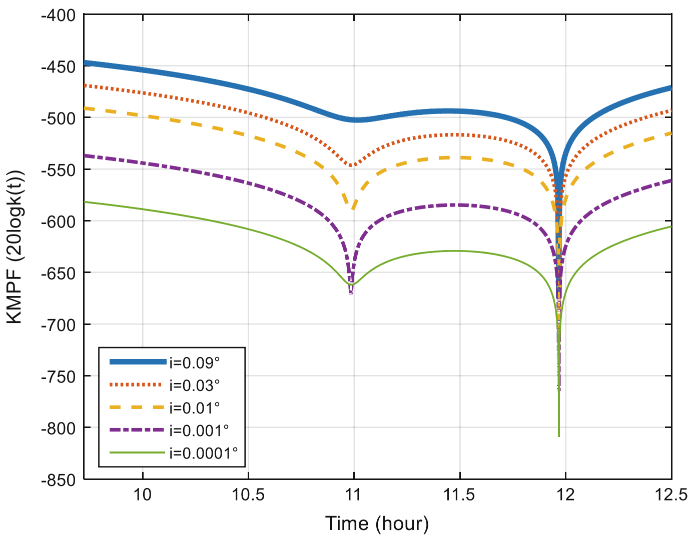

Fig. 4 Fading curve of KMPF

(iii) When $i = 0.09^\circ$ and $i = 0.0001^\circ$, the amplitudes of KMPF factor show a gentle appearance compared with other circumstances at the first nulling.
(iv) The second nulling of all the curves appears at about 12 h.

In order to thoroughly analyze the impact of the inclination i and eccentricity e on KMPF factor, some conclusions can be summarized by comparing with the corresponding curves trend between Figs. 4 and 5. The normalized curves in Fig. 5 derived from Eq. (11), indicate the trends of satellites' speed in ECEF coordinate system. The analyses based on the above four features are shown as follows:

Feature (i) illustrates that the first nulling of KMPF factor curves is closely related to the inclination i. Moreover, in Fig. 5, at the corresponding location to the first nulling, these five curves show an extreme point, which is the reason for the first nulling of KMPF factor curves.

As feature (ii) and (iii) described, by comparing the five curves in Fig. 5, the fading amplitude of the first nulling of KMPF factor curve does not become greater with increase in the inclination. When inclination becomes larger $(i = 0.09^\circ)$ or smaller $(i = 0.0001^\circ)$, the trend of KMPF factor curve at first nulling is gentle. Nevertheless, when $i = 0.001^\circ$, the fading amplitude of the first nulling reaches maximum. By referring Fig. 5, it can be seen that the sharper curve V fades, the larger fading amplitude goes.

Feature (iv) shows the relationship between the curve V and eccentricity e. if $e = 0$, namely the orbit is a standard circle, the movement of satellite will not affect the range rate between the GEO satellites and receiver and the second nulling will vanish from the KMPF factor curve. The fading amplitude of the second nulling is proportional to the eccentricity e.

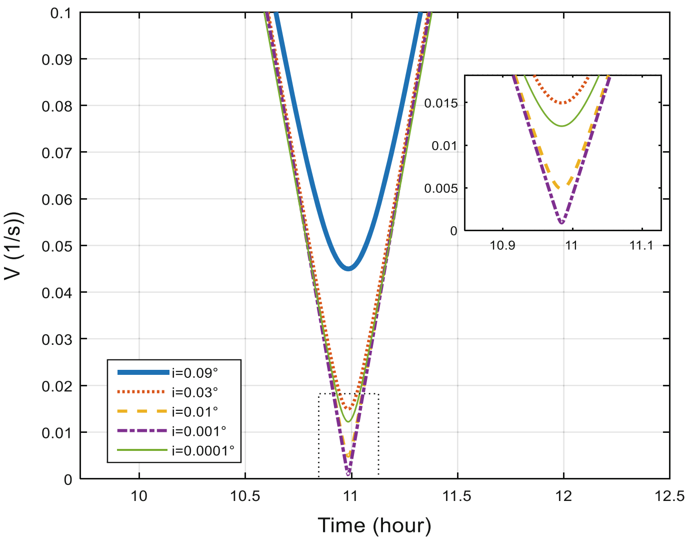

Fig. 5 Relationship between inclination angle and normalized V

4.2.2 Influence of the Argument of Perigee ω on KMPF

As mentioned above, Eq. (11) reflects the relationship between trend of satellite speed and the Kepler orbit parameters, and the first nulling is really close to the trend curve V of the satellite velocity. The further discussions of the location of the first bulling are given below:

Figure 6 shows two KMPF factor curves, and they are plotted by same orbit parameters but the argument of perigee ω. When $\omega = 2\,\text{rad}$, the first nulling appears at the 6th hour and the 18th hours, respectively. However, for $\omega = 0\,\text{rad}$, the first nulling occurs at the 10th hour and the 22nd hours, respectively. Hence, the argument of perigee ω can affect the location of the first nulling. Moreover, the cycle of the first nulling fading is about 12 h, which is affected by the angular rate of satellites in orbit plane ω^s, and is inversely proportional to ω^s.

4.2.3 The Relationship Between of the Variable V, Pseudorange $r(t)$ and KMPF

As discussed in above sections, a detailed analysis about KMPF has been developed by selecting different Kepler orbital parameters. This section will research the relationship between of the variable V, pseudorange $r(t)$ and KMPF. The simulation data of curves plotted in Fig. 7 received in Kiri region on August 29th, 2015 and downloaded from the International GNSS Service (IGS) website. The upper panel in Fig. 7, shows the trend of the variable V and the pseudorange $r(t)$ between the NO. 4 GEO satellite and observation point in Kiri region. The lower panel is

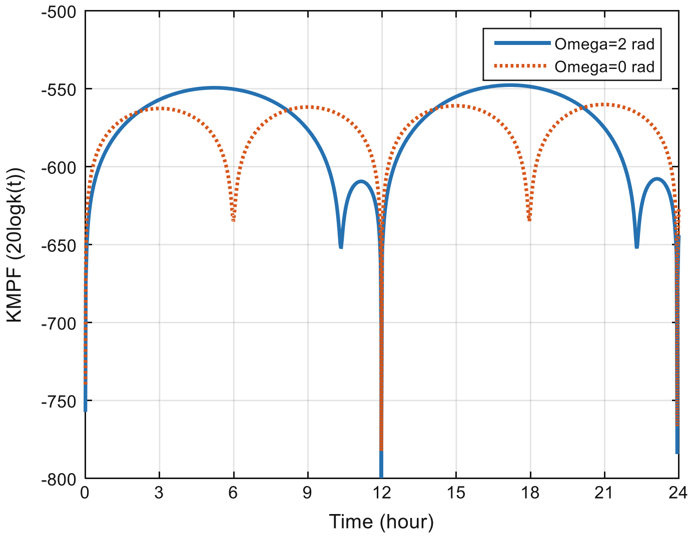

Fig. 6 Relationship between argument of perigee ω and KMPF

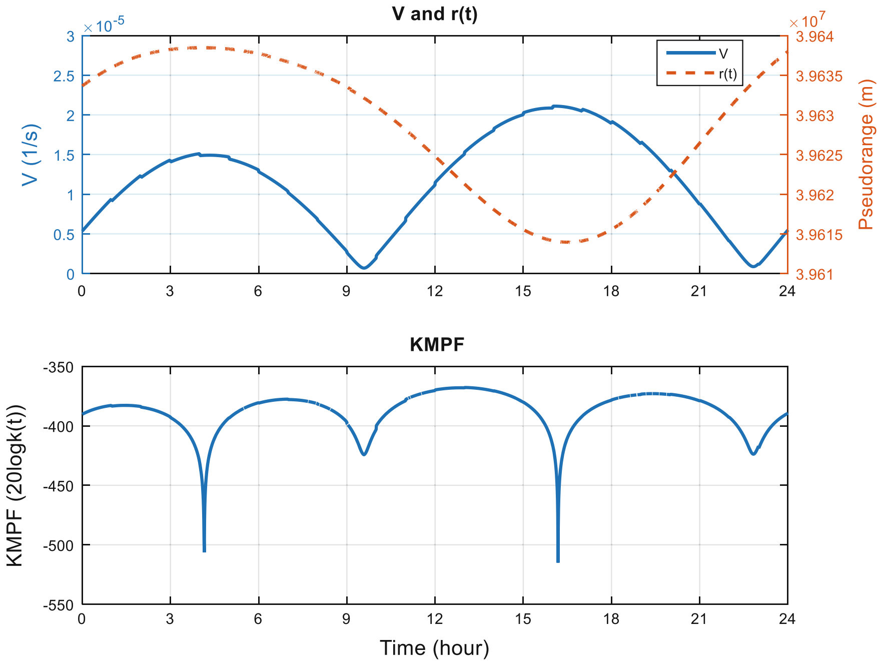

Fig. 7 Relationship between KMPF and pseudorange $r(t)$ and variable V

sketched by the real satellite ephemeris parameters. By analyzing the Fig. 7, some conclusions can be summarized as follows:

(i) The location of the first nulling of KMPF curve is corresponding to the position where the curve V appears the minimal value.

(ii) When the curve V goes to the maximal value, KMPF curve will appear the second nulling, meanwhile the $r(t)$ will show the minimal or maximal value around the position of the second nulling.

5 Simulation Results

This section will verify the theoretical analysis of KMPF factor by simulation. In this simulation, the multipath error envelop curve and Kepler orbit parameters are extracted from data which is received from the real scene at kiri region on August 29th, 2015. The multipath errors on NO. 1 GEO satellite have been calculated by the method mentioned in [7], and this real result is also a reference standard to the simulation.

The top panel in Fig. 8 is a simulation multipath errors, which is based on the ground multipath reflect model proposed in this paper. The middle panel is the real

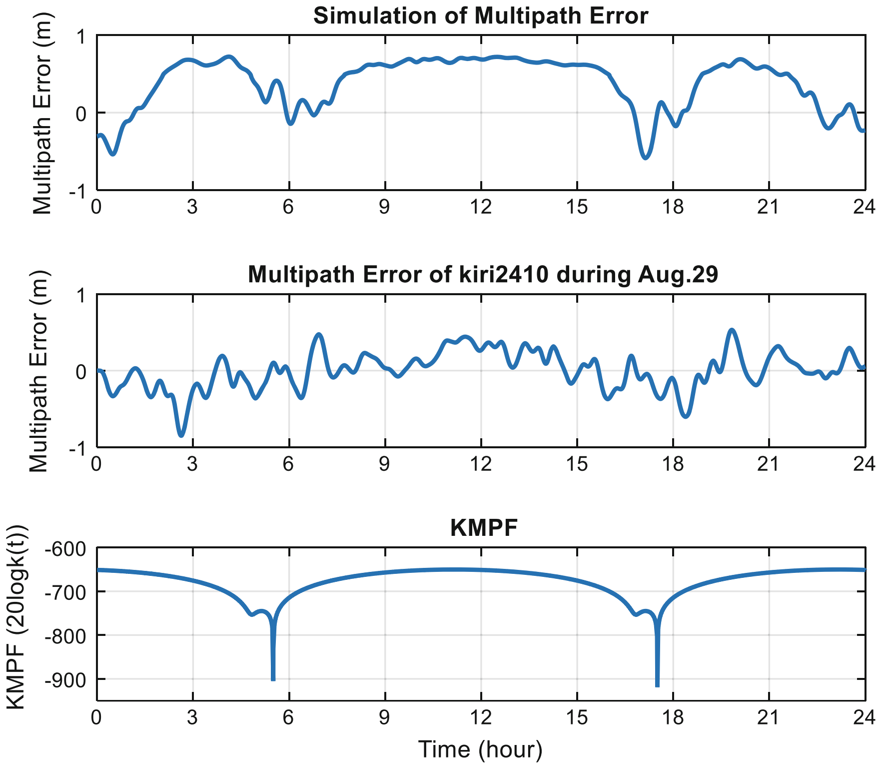

Fig. 8 Characters of multipath of BeiDou NO. 1 GEO

multipath error envelop and the bottom panel is the KMPF factor curve which is plotted by the ephemeris parameters of NO. 1 GEO satellite. According to Eq. (2), GEO satellites multipath effect should present a fixed bias errors, which is called "standing multipath" in [1], and the upper panel also shows this feature.

This article has studied only one reason that may cause the multipath error, the multipath error is related to many factors. Moreover, in a real scene, multipath error is related to many factors, so there exists certain deviation between the simulation curve and practical multipath error curve. However, from the overall trend of these curves, it can be verified that the simulation curve has a certain reference value. The bottom panel shows the waveform of KMPF factor, where the first nulling is not obvious, which means the trend of satellite velocity does not appear large attenuation caused by orbit inclination *i*. The appearance of the second nulling is caused by eccentricity *e*. Lastly, comparing the three curves shown in Fig. 8 in a vertical way, when fading in the KMPF waveform occurs, fluctuation in the multipath error appears. So, this verifies the analysis for the multipath effect in this paper.

6 Summary

In order to research the multipath fading effects of GEO satellites, this article analyzes a reason for GEO multipath by building a ground reflect model. In addition, this article deduces the KMPF equation from the multipath fading frequency formula. Finally, some discussions and simulations about GEO satellites orbit parameters are shown as follows:

(i) The first nulling of KMPF factor is related to the inclination i. When i becomes larger or smaller, such as $i > 0.09^\circ$ or $i < 0.0001^\circ$, the trend of first nulling is gentle. But, when i is around 0.001°, the fading amplitude of first nulling becomes lager.

(ii) The location of first nulling of KMPF factor has a relationship with the argument of perigee ω.

(iii) The second nulling of KMPF is mainly related to the eccentricity e, which is in proportion to the eccentricity e.

(iv) When the curve V goes to the maximal value, KMPF curve will appear the second nulling, meanwhile the $r(t)$ will show the minimal or maximal value around the position of the second nulling.

(v) By comparing the simulation multipath error curve and the real multipath error curve, it can be verified that the KMPF factor has a certain reference value for GEO multipath effects.

Acknowledgments This work was supported by the National Natural Science Foundation of China (contract no. 61301094) and BeiDou Special Fund (contract no. GFZX0301040115).

References

1. Timothy S, Jason B, Arthur R (2008) WAAS benefits of geo ranging. In: Proceedings of the 21st international technical meeting of the satellite division of The Institute of Navigation (ION GNSS 2008), Savannah, GA, pp 1903–1910
2. Phelts R, Walter T, Enge P, Akos D, Shallberg K, Morrissey T (2004) Range biases on the WAAS geostationary satellites. In: Proceedings of the ION national technical meeting, San Diego, California, pp 26–28
3. Yang G, Xiaowei C, Mingquan L, Hong L, Zhenming F (2012) The analysis and simulation of multipath error fading characterization in different satellite orbits. In: Proceedings of China satellite navigation conference (CSNC). Springer, Heidelberg, pp 297–308
4. Yang G, Zheng Y, Xiaowei C, Mingquan L (2014) Analysing the orbit influence on multipath fading in global navigation satellite systems. IET Radar Sonar Navig 8(1):65–70
5. Guangxing W, Kees de J, Qile Z, Zhigang H, Jing G (2014) Multipath analysis of code measurements for Beidou geostationary satellites. In: GPS Solutions. Springer, Heidelberg, pp 129–139
6. Markus I (2010) Characterization of multipath phase rates in different multipath environments. GPS Solut 14(4):305–317
7. Byun SH, Hajj GA, Young LE (2002) Development and application of GPS signal multipath simulator. Radio Sci 37:10–110–23